Optical Engineering

OpticalEngineering.SPIEDigitalLibrary.org

Simplified physical model of interferometric radius of curvature test using the yybar diagram

Reem Alsalamah
Patrick J. Reardon

SPIE.

Reem Alsalamah, Patrick J. Reardon, "Simplified physical model of interferometric radius of curvature test using the yybar diagram," *Opt. Eng.* **58**(9), 095104 (2019), doi: 10.1117/1.OE.58.9.095104.

Simplified physical model of interferometric radius of curvature test using the yybar diagram

Reem Alsalamah and Patrick J. Reardon*
University of Alabama in Huntsville, Center for Applied Optics Huntsville, Alabama, United States

Abstract. The yybar diagram for Gaussian beam optics is employed to model the behavior of an interferometer system testing very small radius parts. The model was developed to overcome the limitations and known inconsistencies of a paraxial optics representation used to evaluate a calibration method for testing cylindrical wave optics using a fiber reference test. Gaussian beam analysis inherently contains physical optics conditions, and the yybar diagram method provides both an intuitive and powerful framework to generate analytical solutions. Particularly, we show how to model an interferometric test from a Fizeau transmission sphere (TS), to a small test ball and back to the TS, and yield test ball radius limits as a function of the test wavelength and TS $F/\#$. A computation of error estimates for measuring the radius of curvature of the test balls is also presented. [DOI: 10.1117/1.OE.58.9.095104]

Keywords: optical metrology; radius of curvature; Gaussian beams; yybar diagram.

Paper 190678 received May 17, 2019; accepted for publication Aug. 26, 2019; published online Sep. 17, 2019.

1 Introduction

The fiber reference test employs a specially prepared reflective coated optical fiber as the reference surface for an interferometric test that employs or results in a cylindrical wave.[1–5] A previous paper presented the experimental results of the alignment sensitivities of the fiber reference test when employing a proposed new method for absolute calibration of cylindrical wave metrology.[6] However, in the analysis, paraxial optics methods were employed, which, when investigating the behavior of the converging cylindrical beam very near focus and interacting with a reflecting surface of a small radius (<0.1 mm) are insufficient to describe the physical situation; at cat's eye position, the wavefront does not have a radius of curvature of zero and it was uncertain whether the beam would even have a null position where the wavefront curvature matched the fiber surface curvature. In an effort to improve this analysis, an analytically tractable technique that employed physical optics was sought. The result was to employ Gaussian beam optics to utilize the yybar diagram method of laser beam representation to perform the analysis. This paper presents the approach and some readily deduced characteristics of interferometrically testing small radius parts. The analysis, presented here assuming rotational symmetry, yields a relationship that defines the boundary between conditions where the fiber test may yield one or two separate positions where the small radius reference surface will produce null fringes depending on the test wavelength, the convergence of the test beam, which defines the size of the waist it would form, and the radius of the test surface. This paper begins by briefly describing the yybar diagram, focusing on the properties of specific use with regards to Gaussian beam analysis used in this paper. The geometry and goals of the experiment are then described, and the yybar diagram is used to derive the results. The paper concludes with a brief analysis showing the impact on the well-understood radius test and a description of subsequent work to follow.

*Address all correspondence to Patrick J. Reardon, E-mail: patrick.reardon@uah.edu

2 Simple Physical Methods

2.1 *yybar Diagram*

The yybar diagram[7,8] was developed as a graphical representation of geometrical paraxial optics by Delano. One plots the paraxial chief ($\overline{y}$) and marginal (y) ray heights at each surface as they are sequentially encountered through the optical system. From the plot, one can visually infer much information about the system and the individual components that form it, and there are simple algebraic equations that allow for precise numerical evaluations of the system (Fig. 1).

2.2 *Modeling Gaussian Beams with the yybar Diagram*

The yybar method was first applied to laser beam propagation by Kessler and Shack.[9] To make the correspondence, consider that a Gaussian beam can be represented by two rays; a divergence ray and a waist ray (Fig. 2), both of which follow all the standard paraxial ray optics relations for refraction and translation.

We arbitrarily define the height of the waist ray as y and the height of the divergence ray as $\overline{y}$ and plot the result (Fig. 3).

In the same way that paraxial optics parameters can be inferred graphically from the yybar diagram so can Gaussian beam parameters. A primary one is the location of the beam waist. In Fig. 3, the red dashed line represents the propagating Gaussian beam. The beam waist is located where $\overline{y} = 0$, which is also where the line is closest to the yybar origin. The beam waist size, *wo*, is defined by the smallest distance from the line to the yybar diagram origin. Or, the beam waist is located where the line is tangent to a circle centered on the origin, and its size is the radius of the circle.

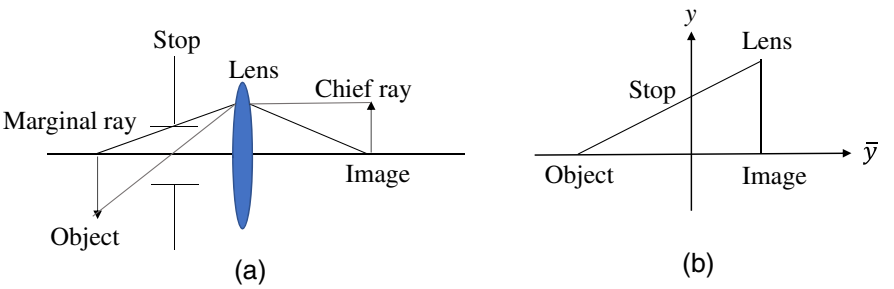

Fig. 1 (a) Marginal and chief rays given a simple lens with the stop near the FFP. (b) The yybar diagram for the same lens system.

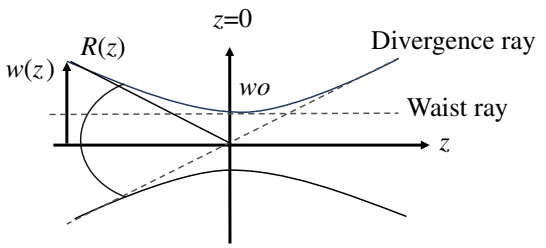

Fig. 2 Gaussian beam $1/e^2$ point curves shown near waist, with divergence and waist rays indicated.

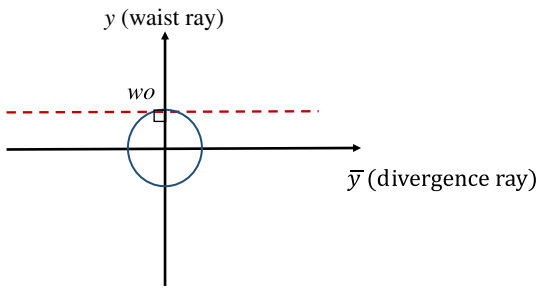

Fig. 3 A yybar diagram, red dashed line, for the propagating beam in Fig. 2, Note that line is tangent to blue circle of radius *wo*.

There are also a number of simple relations that can be used to compute various parameters for the propagating beam. First, the beam size can be computed at any point along the propagating beam using the following equation:

$$w = \sqrt{\overline{y}^2 + y^2}. \tag{1}$$

Distances between two points, $(\overline{y}o, yo)$ and $(\overline{y}1, y1)$, along a segment defining the propagating beam is calculated using the following equation:

$$t = \frac{1}{L}\begin{vmatrix} yo & \overline{y}o \\ y1 & \overline{y}1 \end{vmatrix}, \tag{2}$$

where L is the LaGrange invariant, which, for the laser beam propagation model, is computed as

$$L = \frac{\lambda}{\pi} = n\overline{y}u - ny\overline{u}, \tag{3}$$

where λ is the laser wavelength and, when divided by π, sets the value of L.[9] As also shown in Eq. (3), L is related to the barred and unbarred values as with geometrical optics, where u and $\overline{u}$ are the ray angles for two rays. The radius of curvature of the beam's wavefront in yybar diagram is given by

$$R(\overline{y}, y, \overline{u}, u) = \frac{y^2 + \overline{y}^2}{\overline{y}\,\overline{u} + yu}. \tag{4}$$

Note that Eqs. (2) and (3) are identical and similar, respectively, compared to those used in the yybar diagram for paraxial optics. As an example, $R(\overline{y})$ and $w(\overline{y})$ for a propagating Gaussian beam in vacuum of $\lambda = 632.8$ nm, $wo = 0.0031$ mm, and represented as in Fig. 3 are calculated and plotted in Fig. 4. To compute, $R(\overline{y})$ requires $\overline{u}$ and u.

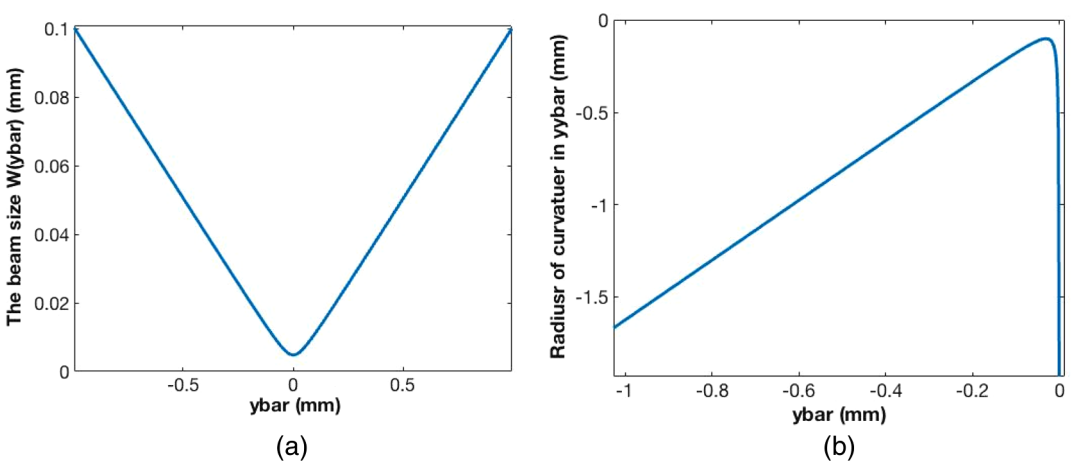

Fig. 4 (a) The beam width, $w(\overline{y})$, through the waist and (b) radius of curvature, $R(\overline{y})$, up to the waist for the Gaussian beam in Fig. 3.

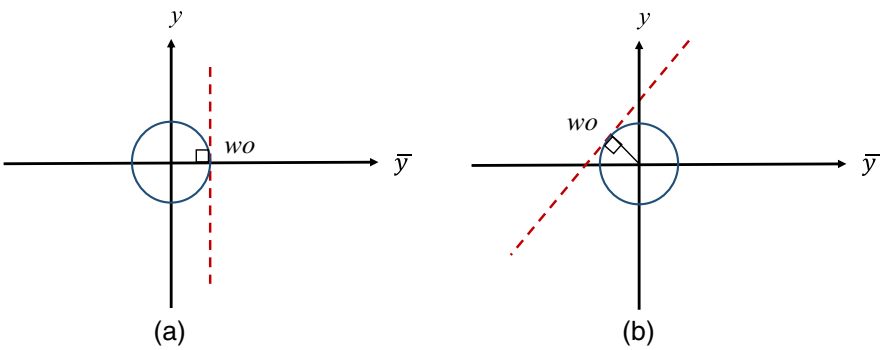

Fig. 5 Different yybar representations of the same Gaussian beam of waist radius of *wo*.

We choose to define the beam from the transmission sphere (TS) to have $y = wo$ and $u = 0$ (Fig. 3) so from Eq. (3), $\overline{u} = \frac{L}{y} = \frac{\lambda}{\pi wo}$. The plots for the Gaussian beam size and radius of curvature, Fig. 4, should be recognizable.[10] $\overline{y}$ is directly related to propagation distance, z, through Eq. (2) yielding $z = \frac{\pi wo\overline{y}}{\lambda}$. We note here that, throughout this paper, examples are based on a red HeNe laser system with a 100-mm diameter $F/7.6$ TS, which we define to have $wo = 0.0031$ mm at its focus.

One final critical difference between the yybar representation of propagating laser beams and paraxial optics is that the meaning of the yybar diagram for laser beam propagation is unchanged when the traces are rotated about the origin. Figure 5 shows two representations of the same propagating beam with a beam waist *wo*. Numerically, they only differ in how the two rays are defined; Fig. 5(a) flips the ray definition set in Fig. 3, and in Fig. 5(b), neither y nor $\overline{y}$ is the waist or divergence ray.

3 Interferometric Test Modeled with the yybar Diagram

3.1 *Geometry of the Interferometric Test*

The interferometer configuration analyzed in this paper consists of a Fizeau system from TS to the reference sphere under test, a small reflective sphere of radius *rb*, where it reflects and then returns to the TS (Fig. 6). Position of the ball, z, is defined by the location of the convex ball surface relative to the beam waist produced by the TS, where $z = 0$ when they are coincident. Since the ball surface has power, the reflected Gaussian beam may have a different divergence, waist size, and waist location.

3.2 *Analysis of Interferometric Test*

The goal of this model is to analyze where the test ball must be to yield null fringes. Logically, this will occur if the reflected beam re-entering the TS meets two constraints: it has the same beam size and the same radius of curvature that the beam had when it initially exited the TS, $w_{TS} = w_{TS}{}'$ and $R(z_{TS}) = R(z_{TS})'$ where the primes indicate the beam after reflection from the reference ball. If this condition is met, one can also state that the reflected beam waist size and position must be identical to the initial beam waist size and position for the beam from the TS, $wo = wo'$ and $w(0)' = wo$. For simplicity, we again define the beam from the TS as a horizontal line of height *wo*. The TS beam, red lines in Fig. 6, interacts with the test surface at some position z measured from the incident beam waist, which is located at $(\overline{y}, y) = (0, wo)$. Since the divergence and waist rays still follow the laws of paraxial optics, the waist ray, $u = 0$, will virtually go to a height of zero at the front focal point (FFP) of the convex ball a distance $\frac{-rb}{2}$ from the reflecting surface. Since we also know $\overline{u}$, the value of $\overline{y}$ at the FFP is

$$\overline{y}F = \left(\frac{-rb}{2}\right)\left(\frac{\lambda}{\pi wo}\right) = \left(\frac{-rb\lambda}{2\pi wo}\right), \tag{5}$$

which is independent of where the reference ball is located in z. We denote the test ball position as $(\overline{y_p}, y_p) = (\overline{y_p}, wo)$. Thus, the segment that represents the reflected beam is along a line that passes through $(\overline{y}F, 0)$ and the reference ball location, $(\overline{y_p}, wo)$. As described above, to find the locations for the test ball that produces a null fringe requires the reflected beam to have the identical beam waist size and location as the beam from the TS.

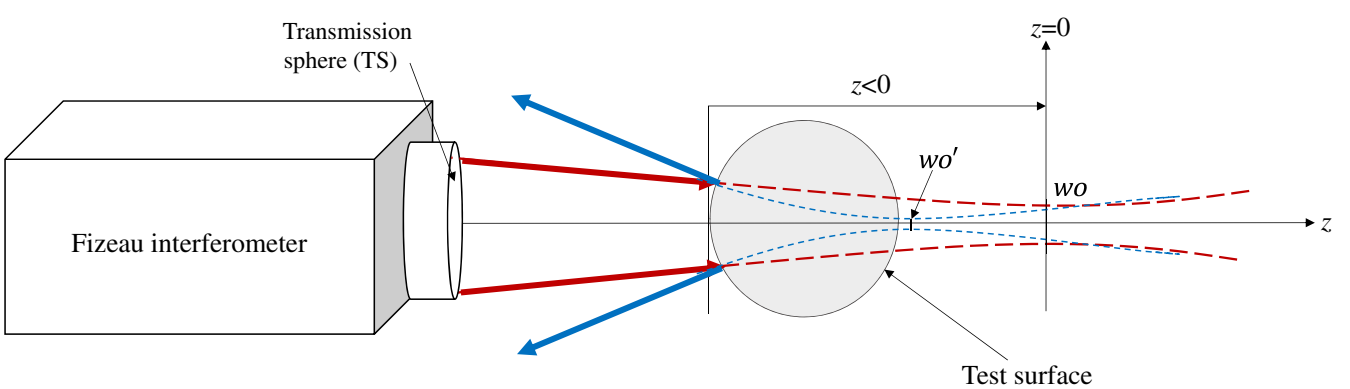

Fig. 6 The interferometer system being modeled, from TS to test ball back to TS.

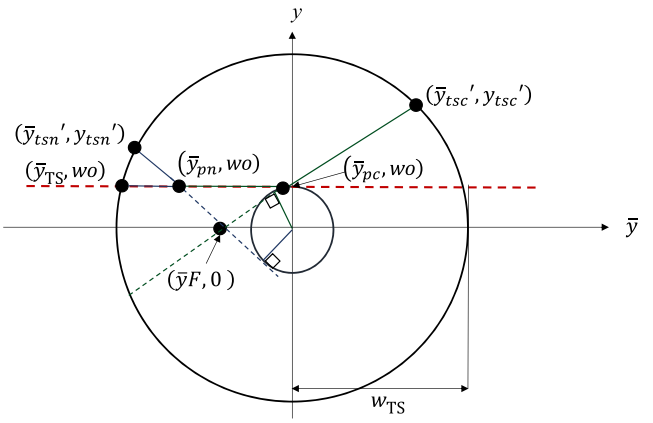

Fig. 7 The yybar diagram for both the null and cat's eye positions, from TS to test ball back to TS'.

To ensure the first constraint, the reflected beam must be on a line that is tangent to the centered circle of radius wo. After some algebra, this results in the following equations for deriving two $\overline{y_p}$, values:

$$\bar{y}_{pn} = \bar{y}F - \sqrt{\bar{y}F^2 - wo^2}, \tag{6}$$

$$\bar{y}_{pc} = \bar{y}F + \sqrt{\bar{y}F^2 - wo^2}, \tag{7}$$

where $y_{pn} = y_{pc} = wo$ (Fig. 7).

These are the well-known null and cat's eye positions—$(\bar{y}_{pn}, y_{pn})$ and $(\bar{y}_{pc}, y_{pc})$.[11] But at this point, we have only met one of the requirements stated above: $wo = wo'$. We prove that the other condition is automatically met based on the properties of the yybar diagram. Since the reflected and incident beams are both represented by lines tangent to the same circle, and the test ball position is located at the two lines' intersection, and the initial and reflected waists are located at the tangent points of the lines, the area of triangle $[(0, 0), (0, wo), (\bar{y}_p, wo)]$ is identical to the area of triangle $[(0, 0), (\bar{y}_{wo}, y_{w0}), (\bar{y}_p, wo)]$ (Fig. 8). In a yybar diagram, this means the distances are identical and therefore the incident and reflected beam waists are located at the same position; both requirements for null fringes are met. The identical waist positions can also be derived algebraically using Eq. (2), computing the distance from the TS to the ball, and then from the ball back to the TS, or the distances from the ball to the incident and reflected waists.

Also note that Eqs. (6) and (7) reveal that when $\bar{y}F = wo$, there is only one solution. We define this as the minimum test ball size, using Eq. (5) and $\bar{y}F = wo$,

$$rb\ \min = \frac{2\pi w0^2}{\lambda}. \tag{8}$$

When $\bar{y}F < wo$, Eqs. (6) and (7) yield imaginary values for $\bar{y}_p$; there is no solution for this case. This is readily observed from the yybar diagram since any beam represented by a line that passes through a point inside the circle of radius wo cannot have a beam waist size of wo, thus the two constraints cannot be met. We must redefine what constraints should be met to achieve a null fringe when the ball radius is below the minimum defined by Eq. (8). One approach is that only the radius of curvature of the reflected beam at the TS needs to match the radius of curvature of the initial beam at the TS. By equating the distances from the TS to the ball, and from the ball back to the TS, and then also making Eq. (4) match for the beam first leaving and then entering the TS after reflection, we find that the solution is that the reflected beam is represented by a ray parallel to the y axis, or $\bar{y} = \frac{-rb\ \min}{2}$. Note that now, the divergence and waist rays are defined by y and $\bar{y}$, respectively. The location of the reflected TS is such that the beam size (w') is far larger than when the beam exited the TS, so the contrast of the fringes will be lower. This is again evident based on the area of triangles; the distance from the TS to the ball is measured along the line $y = wo$, but back to TS$'$ along $\bar{y} = x$, where $x < wo$. To match areas, $\bar{y}_{ts}{}' \sim \bar{y}_{ts} \times \frac{wo}{x}$, and since both $\bar{y}_{ts}{}'$ and $\bar{y}_{ts}$ are far larger than $y_{ts} = wo$ and $\bar{y}_{ts}{}' = x$, respectively, $w_{ts} \sim \bar{y}_{ts}$ and $w_{ts}{}' \sim \bar{y}_{ts}{}'$. So, if $\bar{y}F = \frac{wo}{2}$, $w_{ts}{}' \sim 2w_{ts}$. One final point to note is that this analysis shows how the accuracy of the standard method for determining the radius of curvature of a surface, measuring the distance between the null and cat's eye positions,[12] rapidly degrades as the radius approaches the minimum. For example, Fig. 9 is a plot of the absolute percent error in logarithmic scale $(100[\frac{\text{actual}-\text{measured}}{\text{actual}}])$ given the $F/7.6$ TS used throughout this paper.

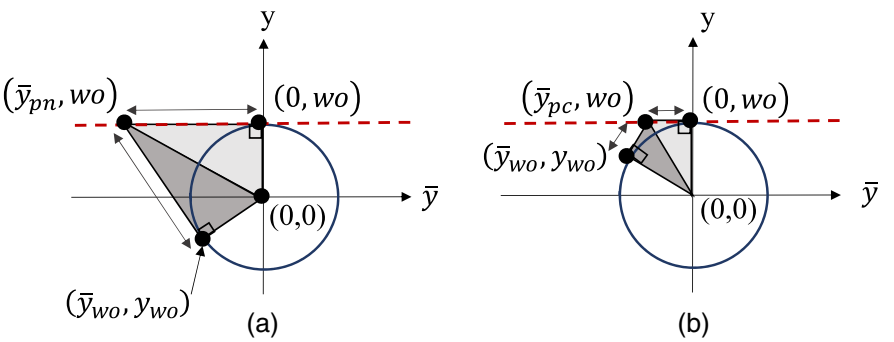

Fig. 8 Area is proportional to distance in a yybar diagram, so the triangles show the distance from the ball surface to the incident or reflected waist is identical for the (a) null or (b) cat's eye position; the reflected and incident waists are coincident.

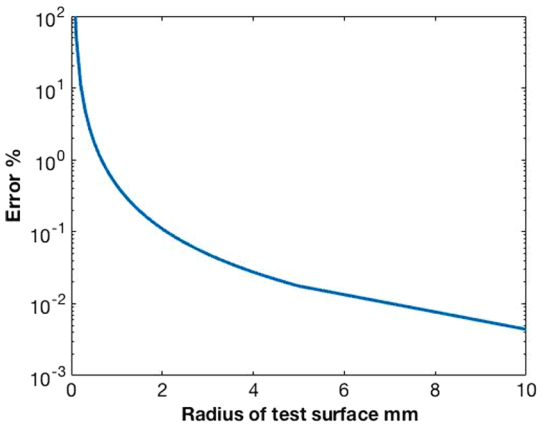

Fig. 9 The percent error in logarithmic scale of the measured radius of curvature using the null to cat's eye test.

For reference, radii of 2, 0.6, 0.2, and 0.093 mm yield percent errors of 0.1%, 1%, 10%, and 100%, respectively.

4 Conclusion

This paper has presented a physical optics-based analysis of an interferometric test of a small radius test part. The yybar diagram method for Gaussian beams provides simple, visually evident results as well as analytical relations. The method has found tractable results: defining a minimum surface radius with only one null fringe position and determining measurement error when finding radius of curvature with the null/ cat's eye test, given a test wavelength and TS $F/\#$. Using this framework, a subsequent paper will show how calibration of TSs using small radius reference spheres and the cylindrical nulls using a fiber reference can be modeled, including a detailed analysis of the misalignment errors in these tests.

Acknowledgments

We are thankful to King Saud University in Riyadh and the Saudi government for their support to pursue a PhD in the Optical Science and Engineering Program, and grateful the Center for Applied Optics at the University of Alabama in Huntsville for providing laboratory space and facilities.

References

1. J. Geary and L. Parker, "A new test for cylindrical optics," *Proc. SPIE*, **661**, 359–364 (1986).
2. J. Geary, "Data analysis in fiber optic testing of cylindrical optics," *Opt. Eng.* **28**(3), 283212 (1989).
3. J. Geary, "Fiber/cylinder interferometer test: focus and off axis response," *Opt. Eng.* **30**(12), 1902–1909 (1991).
4. J. Geary, "An overview of cylindrical optics testing using a fiber optic reference," *Proc. SPIE* **2536**, 68–74 (1995).
5. F. Liu et al., "Analyzing optics test data on rectangular apertures using 2-D Chebyshev polynomials," *Opt. Eng.* **50**, 043609 (2011).
6. A. Alatawi, P. J. Reardon, and F. Liu, "Fiber reference misalignment induced error in cylindrical wave interferometry," *Opt. Express* **23**(12), 15405 (2015).
7. E. Delano, "First order design and the yy diagram," *Appl. Opt.* **2**, 1251–1256 (1963).
8. R. V. Shack, "Analytic system design with pencil and ruler the advantages of the yy diagram," *Proc. SPIE* **39**, 127–140 (1973).
9. D. Kessler and R. V. Shack, "yy diagram, a powerful optical design method for laser systems," *Appl. Opt.* **31**, 2692–2707 (1992).
10. B. E. A. Saheh, *Fundamental of Photonics*, 2nd ed., pp. 74–86, John Wiley& Sons, Hoboken, New Jersey (2007).
11. K. Creath and J. Wyant, "Testing spherical surfaces: a fast, quasi-absolute technique," *Appl. Opt.* **31**(22), 4350–4354 (1992).
12. J. Geary, *Optical Testing*, pp. 92–94, Willmann-Bell Inc., Richmond, Virginia (2012).

Reem Alsalamah is currently pursuing her PhD in optics science and engineering at the University of Alabama in Huntsville. She is a member of SPIE.

Patrick J. Reardon is the director of the Center for Applied Optics of Alabama in Huntsville. His research has covered the fields of optical design, fabrication, and testing for Department of defense, aerospace, ophthalmic, and commercial applications.